Liquid Crystals
Publication details, including instructions for authors and subscription information:
http://www.informaworld.com/smpp/title~content=t713926090

The discotic mesophases of octaalkyloxy-and octaalkanoyloxyorthocyclophanes

N. Spielberg[ab]; M. Sarkar[a]; Z. Luz[b]; R. Poupko[b]; J. Billard[c]; H. Zimmermann[d]
[a] Department of Physics, Kent State University, Kent, Ohio, U.S.A. [b] The Weizmann Institute of Science, Rehovot, Israel [c] Laboratoire de Physique de la Matière Condensée, Collège de France, Paris, France [d] Max-Planck-Institut für Medizinische Forschung, Heidelberg, Germany

To cite this Article Spielberg, N. , Sarkar, M. , Luz, Z. , Poupko, R. , Billard, J. and Zimmermann, H.(1993) 'The discotic mesophases of octaalkyloxy-and octaalkanoyloxyorthocyclophanes', Liquid Crystals, 15: 3, 311 — 330
To link to this Article: DOI: 10.1080/02678299308029134
URL: http://dx.doi.org/10.1080/02678299308029134

LIQUID CRYSTALS, 1993, VOL. 15, NO. 3, 311–330

The discotic mesophases of octaalkyloxy- and octaalkanoyloxyorthocyclophanes

by N. SPIELBERG†‡, M. SARKAR†, Z. LUZ‡*, R. POUPKO‡, J. BILLARD§ and H. ZIMMERMANN¶

‡ The Weizmann Institute of Science, 76 100 Rehovot, Israel
† Department of Physics, Kent State University, Kent, Ohio 44242, U.S.A.
§ Laboratoire de Physique de la Matière Condensée, Collège de France, Paris, France.
¶ Max-Planck-Institut für Medizinische Forschung, AG Molekülkristalle, Jahnstrasse 29, 6900 Heidelberg, Germany

(*Received 27 January 1993; accepted 1 May 1993*)

The mesomorphic properties of 3,4,10,11,17,18,24,25-octaalkyloxy and octaalkanoyloxycyclotetraveratrylene (orthocyclophane) have been investigated by differential scanning calorimetry (DSC), polarizing optical microscopy, NMR and X-ray diffraction. Twelve homologues of the octaalkyloxy series, with equal side chains containing $n = 5$ to 16 carbons per side chain, were studied and found to be mesomorphic with at least one columnar mesophase. All members of the series exhibit a biaxial columnar mesophase denoted by D_1. The homologues, with $n = 10$ to 16, also exhibit a uniaxial columnar mesophase, between the D_1 and the liquid phase, which is denoted by D_2. Miscibility studies show that the D_1 phases of all the compounds, and the D_2 mesophases of the high members of the series are isomorphic. The D_1 and D_2 phases are completely miscible with M_1 and M_2 of the hexaalkanoyloxytriphenylene series respectively. They may, therefore, be classified as discotic B and discotic A respectively. Both phases remain stable upon addition of substantial amounts of non-mesogenic aromatic compounds. The transition between D_2 and D_1 is weakly first order (not observed by DSC), but the interconversion is spread over a wide temperature range ($\sim 20°C$ for the $n = 13$ homologue). The analysis of the X-ray results shows that D_2 is hexagonal and that D_1 is rectangular, with one and two molecules per unit cell respectively. The lattice parameters for all measured compounds in the two mesophases are reported.

Four homologues of the octaalkanoyloxy derivatives of cyclotetraveratrylene with side chains containing 12, 14, 15 and 16 carbons were also studied by X-ray diffraction. These compounds exhibit a single discotic columnar mesophase with essentially rectangular symmetry.

1. Introduction

In recent years, several new homologous series of discotic mesogens, based on cycloveratrylene condensation products, have been synthesized and their liquid crystalline properties studied. The first of these new series were the so-called pyramidic liquid crystals consisting of substituted tribenzocyclononatriene (cyclotriveratrylene) [1–4]. Subsequently it was found that substituted orthocyclophane (cyclotetraveratrylene) [5, 6] and the related metacyclophane series with eight or twelve side chains [7–10], as well as dimers and polycondensates of ether derivatives of orthocyclophane,

* Author for correspondence.

0267–8292/93 $10·00

linked via α, ω-dicarboxylic spacers [11], may also be mesogenic. More recently, the study of the octaalkyloxyorthocyclophanes was extended by Percec and co-workers [12–14], who also described mesomorphic polycondensates of these monomers linked via α, ω-diether spacers.

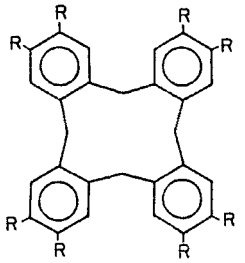

CTTV-I-*n*, $R = C_nH_{2n+1}O$

CTTV-II-*n*, $R = C_{n-1}H_{2n-1}COO$

In the present work we describe additional measurements made with the mesophases of the octaalkyloxy and octaalkanoyloxyorthocyclophane series, henceforth referred to as CTTV-I-*n* and CTTV-II-*n*, respectively (for cyclotetraveratrylene symmetrically substituted with $C_nH_{2n+1}O$ or $C_{n-1}H_{2n-1}COO$ side chains). These compounds consist of a highly flexible core [15] with an average four-fold symmetry. We describe phase diagrams obtained by optical microscopy and differential scanning calorimetry (DSC), X-ray diffraction measurements and preliminary deuterium NMR observations. Most of the results concern the CTTV-I-*n* series. They show that the lower members of the series ($n = 5$ to 9) exhibit columnar biaxial mesophases, D_1, with centred or pseudo-centred rectangular symmetry. The higher members of the series ($n = 10$ to 16) are dimorphic, each exhibiting two columnar mesophases; a low temperature biaxial and a high temperature uniaxial phase. The biaxial mesophases are isomorphic with D_1 of the lower members, and all uniaxial mesophases, D_2, of the higher members are likewise isomorphous. The transition between the two mesophases is not detectable by DSC but is clearly observed by optical microscopy and in the X-ray diffraction patterns. The main emphasis in the present work concerns the structure of these mesophases and the nature of the transition between them.

Also described are X-ray studies of the mesophases of four members ($n = 12, 14, 15$ and 16) of the CTTV-II-*n* series. These compounds exhibit only a single columnar mesophase with rectangular symmetry.

2. Experimental

Polarizing optical microscopy (Leitz, Panphot and Zeiss, Universal equipped with a Mettler FP 52 heating stage), differential scanning calorimetry (Mettler, TA 3000) and deuterium NMR (Bruker, CXP300) measurements were performed as described in several earlier publications from our laboratories [5, 6, 16–18]. Likewise the X-ray measurements made with the CTTV-II-*n* series were as described earlier [16, 17] (modified Philips diffractometer, $\lambda = 1{\cdot}5418$ Å). The corresponding measurements for the CTTV-I-*n* series were carried out on a Rigaku powder diffractometer (Dmax-B) with a rotating anode (12 kw, $\lambda = 1{\cdot}5418$ Å) and a graphite monochromator crystal ($2d = 6{\cdot}695$ Å). To reduce the background radiation, the width of the divergence slit was reduced to 0·15 mm and additional anti-scatter slits were introduced in the space between the specimen and the second (Sollar) slit assembly. For the more detailed temperature dependence measurements, the effective height of the slits was reduced to 1 mm to ensure minimal temperature gradients. With this arrangement, scattering

angles as low as 0·5° could be measured, corresponding to a maximum d spacing of about 90 Å. The liquid crystal sample was introduced into standard 1·5 mm o.d. quartz capillaries which were placed into a modified specimen holder. The temperature of the sample was controlled using a specially constructed oven, consisting of two concentric copper cylinders with appropriate apertures for the incident and diffracted X-ray beams. A few turns of heater wire (Evenohm, 0·2 mm, 53·2 ohm m^{-1}) were wrapped around each of the cylinders and connected to a (Omega Engineering Model CN2102-P2) temperature controller, having a nominal resolution of 0·1°C and nominal accuracy of 1·3°C. The temperature sensor (a platinum resistance device) was embedded in the outer wall of the inner copper cylinder. Calibration of the temperature and the temperature gradient was performed using a thermocouple which was inserted into the inner cylinder. The temperatures at the centre of the specimen were within 1°C of the controller reading and the gradients were about 0·7°C cm^{-1}.

The octaalkyloxy (CTTV-I-n) and octaalkanoyloxyorthocyclophanes (CTTV-II-n) were prepared by alkylation and esterification of octahydroxyorthocyclophane (CTTV-OH) respectively. The latter was obtained by condensation of 3,4-dimethoxybenzyl alcohol, followed by cleavage of the methoxy groups using boron tribromide. As an example for the preparation of an ether derivative, that of CTTV-I-10 is described. CTTV-OH (0·5 g) was mixed with ground potassium carbonate (2·5 g), acetone (40 ml) and n-decyl bromide (5 g) in a stainless steel container and stirred for 12 hours while gradually heating to 220°C. This temperature was held for another 48 hours after which the mixture was allowed to cool and the solid KBr and K_2CO_3 separated by filtration. The filtrate was evaporated and the residue was treated with acetone (200 ml), filtered again and evaporated. The solid residue was recrystallized from methylene chloride/ethanol and the product purified by column chromatography (silica, CH_2Cl_2 : n-hexane, 7 : 3), followed by another recrystallization from chloroform/acetone. A yield of 1·1 g, chemically pure (clearing temperature, 143°C) CTTV-I-10 was recovered. Similar yields were obtained for the other members of the series.

Several deuteriated isotopomers of CTTV-I-n homologues, labelled at the crown methylene, the unsubstituted aromatic sites and the α-methylenes of the side chains, respectively, were also prepared. Deuteriation of the core sites was done as described in [4] while deuteriation of the α-methylene was achieved using the corresponding alkyl bromide prepared by standard methods [19].

As an example of the preparation of the CTTV-II-n series, again, that of the $n = 10$ homologue is described. CTTV-OH (0·4 g) was dissolved in warm pyridine. The solution was cooled in an ice bath and decanoyl chloride (8 g) added dropwise, followed by stirring at room temperature for 8 days. The solvent was then removed under vacuum and the residue treated with 10 per cent aqueous hydrochloric acid (300 ml), followed by filtration and two recrystallizations from methylene chloride/ethanol. Further purification was achieved by column chromatography (silica, CH_2Cl_2 : n-hexane, 95 : 5) and a final recrystallization from ethanol, yielding 720 mg of pure CTTV-II-10.

3. Results and discussion

3.1. *Octaalkyloxyorthocyclophane*

3.1.1. *DSC measurements and phase diagrams*

Twelve members of the CTTV-I-n series, with n ranging from 5 to 16, were prepared and their phase diagrams determined by DSC and optical microscopy. The compounds

are stable in the temperature range of the measurements, except for prolonged heating, when decomposition sets in. The transition temperatures and enthalpies are summarized in table 1 and figure 1. These results correspond to (second) heating of crystallized compounds at 1 to 10°C per minute. Usually somewhat lower transition temperatures were obtained on cooling due to supercooling effects. All the homologues studied exhibit several solid phases and at least one discotic mesophase between the solid and the isotropic liquid. The results are very close to those obtained by Percec *et al.* [12, 14]; the main differences are in the identification of some phases as crystalline (C) in the present work, while they were referred to as discotic by Percec *et al.* Also some solid–solid transitions are included in table 1, mainly below room temperature, which were not reported earlier. Our assignment of the phases as crystalline or discotic is based, in addition to the optical microscopy examination, on the X-ray results; when sharp diffraction lines were observed in the 4·0 Å region, the phase was identified as crystalline while their absence was taken as an indication of a mesophase. In general, with increasing side chain length, the melting temperatures decrease regularly with some even–odd effects, while the melting enthalpies seem to increase. For the low members ($n = 5$ to 9) of the series there is just one mesophase (D_1), while there are two (D_1 and D_2) for the higher members ($n = 10$ to 16). The transition between the two mesophases is not observed in the DSC thermograms, as may be seen from the example for CTTV-I-12 in figure 2, but it is very clearly observed in the polarizing optical micrographs and the X-ray measurements to be described below. The clearing temperatures decrease monotonically with n and the corresponding enthalpies seem to be fairly constant throughout the series.

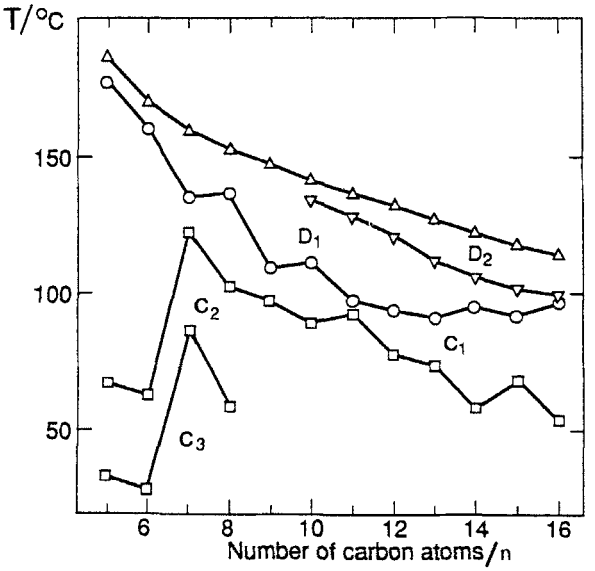

Figure 1. Solid–solid, solid–discotic, discotic–discotic and discotic–isotropic transition temperatures for the CTTV-I-n homologues with $n = 5$ to 16. All transitions were detected by DSC upon (second) heating except for the discotic–discotic transitions (inverted triangles) which were determined by optical microscopy.

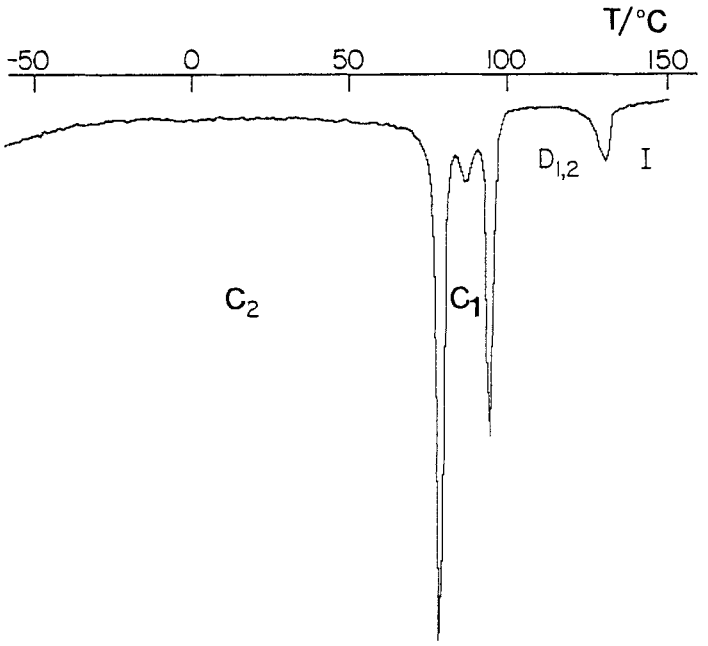

Figure 2. Differential scanning calorimetry (DSC) thermogram of CTTV-I-12 obtained on second heating of the solid. Note the absence of a peak due to the discotic–discotic transition. The weak peak at 87°C is not indicated in table 1.

3.1.2 *Optical microscopy*

The optical microscopy observations were made on thin samples contained between two untreated ordinary glass slips. On heating, several of the solid–solid transitions detected by DSC were also observed under the polarizing microscope as changes in the crystal morphology. Melting to the mesophase was accompanied with rounding off of the crystallites' edges. Pressing the cover slip of the melted crystals with a fine steel needle gave a birefringent viscous paste with a negative optical sign. The clearing temperatures were readily detected by the complete extinction of the field of view.

Slow cooling (0·2°C min^{-1}) of the isotropic liquid gave well developed birefringent domains with a negative optical anisotropy typical of discotic columnar mesophases. The appearance of the optical micrographs was different for the low ($n=5$ to 9) and high ($n=10$ to 16) members of the series. The mesophases formed by the low members exhibit either domains with non-uniform extinction and irregularly curved boundaries, or they exhibit uniform extinction with digitized (finger like) contours (see figure 3(*a*)), depending on the cooling rate. After total transformation, large areas with uniform extinction can be observed (see figure 3(*b*)). In the non-uniform domains, defects with rectilinear axes, characteristic of discotic mesophases, are observed. When viewed with linearly polarized light (analyser removed) the defects disappear when the electric field direction of the beam is set parallel to the defects' axes. In the uniform domains, two kinds of rectilinear defects could be distinguished, being parallel and at 45° to the neutral lines respectively. Under examination with crossed polarizers none of the lower ($n=5$ to 9) members of the series showed normally oriented domains, suggesting that the mesophases of these compounds are optically biaxial. They will be designated as D_1.

Table 1. Phase transition temperatures (°C) and enthalpies (kJ mol^{-1}) for the CTTV-I-*n* series†.

n	C_4		C_3		C_2		C_1		D_1		D_2		I
5	●	−43·1 (15·6)	●	33·2 (12·9)	●	67·5 (14·1)	●	177·0 (54·3)‡	●			186·4	●
6	●	−17·0 (6·5)	●	29·3 (10·0)	●	62·8 (4·8)	●	160·1 (56·1)‡	●			170·0	●
7			●	86·8 (41·6)	●	122·3 (8·5)	●	136·0 (14·1)	●			159·9 (18·1)	●
8	●	6·2 (2·9)	●	69·1 (21·0)	●	103·0 (4·2)	●	137·2 (24·2)	●			153·2 (15·1)	●
9	●			−5·9 (5·6)	●	97·6 (58·4)	●	109·4 (42·0)	●			147·9 (17·8)	●
10	●			−49·3 (4·7)	●	89·6 (35·6)	●	111·9 (33·6)	●	136·6	●	142·0 (15·3)	●
11	●	−37·9 (2·6)	●	17·2 (11·4)	●	93·5 (104·4)‡	●	98	●	128·5	●	137·2 (19·7)	●
12	●				●	78·1 (166·8)‡	●	94·4	●	121·5	●	133·2 (19·5)	●
13	●					74·6 (4.2)	●	91·5 (175·5)	●	112·6	●	127·9 (19·0)	●
14	●					~59§ (~25)	●	96·1 (159·8)	●	106·4	●	123·1 17·8)	●
15	●					~69§ (~9)	●	92·7 (175·2)	●	102·1	●	119·1 (17·0)	●
16	●					~55§ (~25)	●	97·8 (165·0)	●	99·6	●	115·4 (17·3)	●

† The D_1–D_2 transitions are only observed by optical microscopy. All other data are from DSC measurements.
‡ The entry applies to the sum of this and the subsequent transition, since the DSC peaks were not well resolved.
§ Very broad DSC peak.

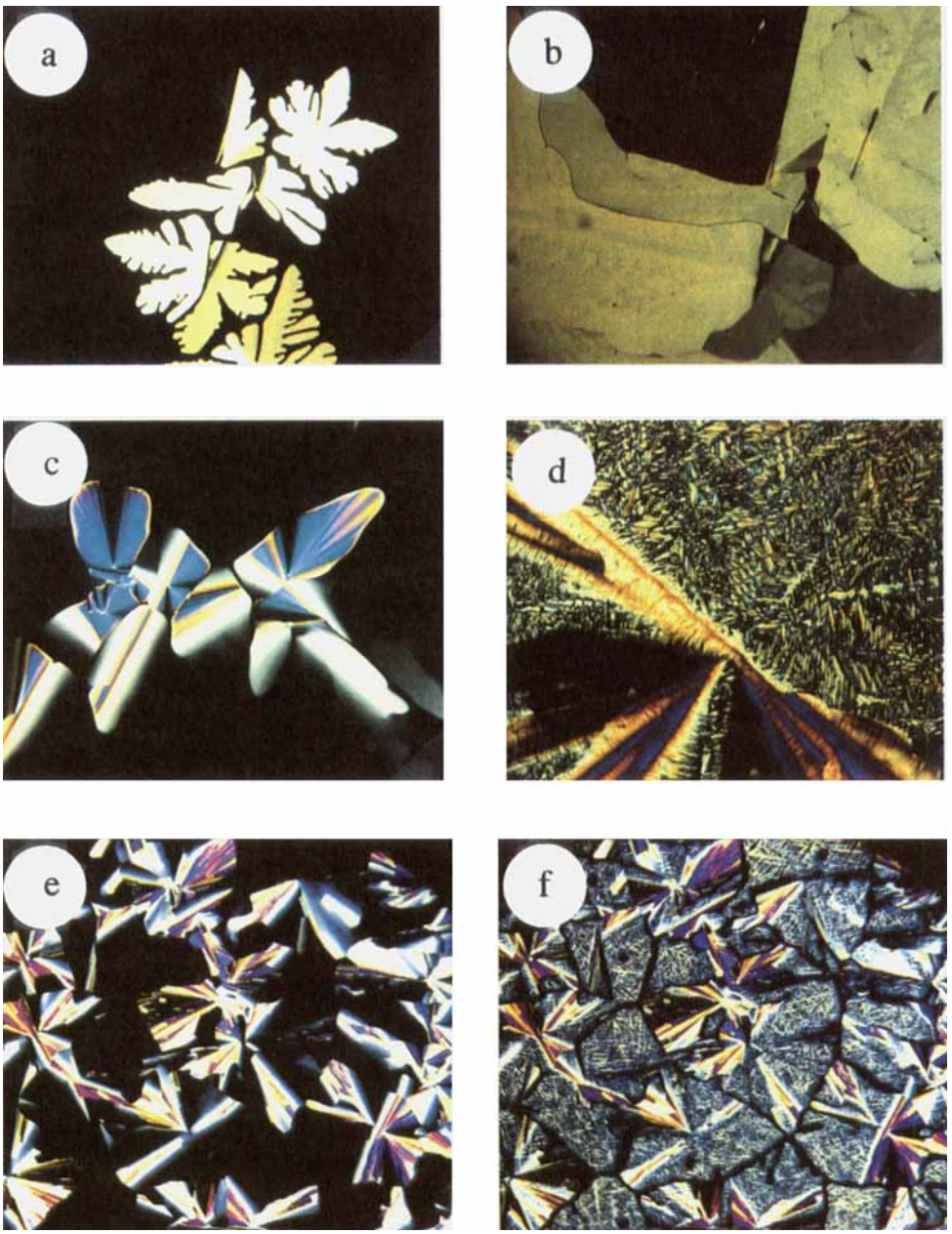

Figure 3. Polarizing optical micrographs. (*a*) D_1 of CTTV-I-7 at 160°C. (*b*) D_1 of CTTV-I-7 at 145°C. (*c*) D_2 of CTTV-I-10 at 137·7°C. (*d*) D_1 of CTTV-I-10 at 123·0°C. (*e*) D_2 of CTTV-I-12 at 122·6°C. (*f*) D_1 of CTTV-I-12 at 121·5°C. In all pictures the polarizing planes are vertical and horizontal with respect to the page edges.

The higher members of the series (with $n = 10$ to 16) also develop, under slow cooling, large uniform domains which exhibit defects with rectilinear axes. However, in these compounds dark areas are often observed (see figure 3 (*c*)) which remain extinguished upon reorientation of the sample between the crossed polarizers. This behaviour is typical of optically uniaxial normally oriented domains and indicates that D_2 is a uniaxial mesophase.

Further cooling of the D_2 mesophase results in a distinct transition which is manifested in the apppearence of elongated birefringent decorations. Two types of such decorations, whose orientations are perpendicular to each other, are observed. Their extinction directions are oblique and in the domains with rectilinear axes, striations perpendicular to the defect axes appear (see figure 3 (*d*)). The textures of the D_1 and D_2 phases are paramorphic and are reproduced upon heating and cooling cycles (see figures 3 (*e*) and (*f*)). The transition is reversible, although some supercooling is detected. For example, for $n = 10$, the low temperature phase appears at 135·8°C upon cooling, while it disappears at 136·6°C upon heating. Thus the transition is apparently first order, but associated with a very low enthalpy, as it is not detected by DSC. This transition was not mentioned in the earlier optical microscopy studies [5, 12], but was subsequently observed by Percec *et al.* [14], in CTTV-I-12 and, as shown in figure 1, it has now been found in all homologues with $n = 10$ to 16.

Optical microscopy studies of contact preparations showed complete miscibility in the liquid and mesophase region of neighbouring homologues of the CTTV-I-*n* series, thus establishing their respective isomorphisms. An example of such a binary phase diagram for the $n = 12$ and $n = 13$ homologues is shown in figure 4. The equilibrium

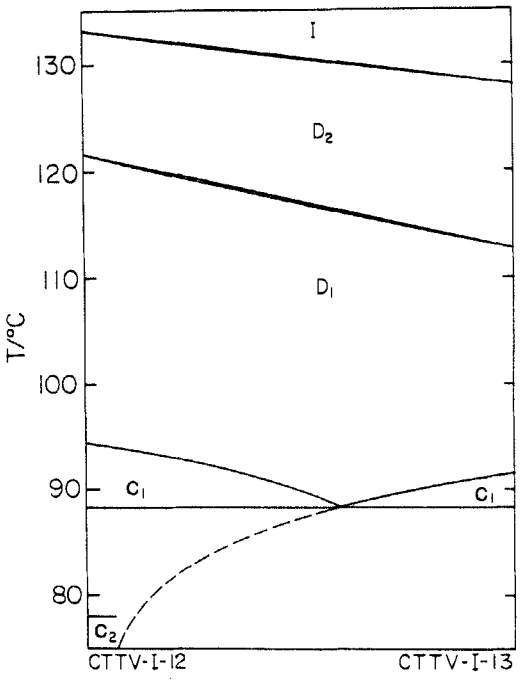

Figure 4. Binary phase diagram of mixtures of CTTV-I-12 (left) and CTTV-I-13 (right). Note the total miscibility of the liquids and the two mesophases. The dashed line is the coexistence curve of the crystals of CTTV-I-13 with the D_1 mesophase.

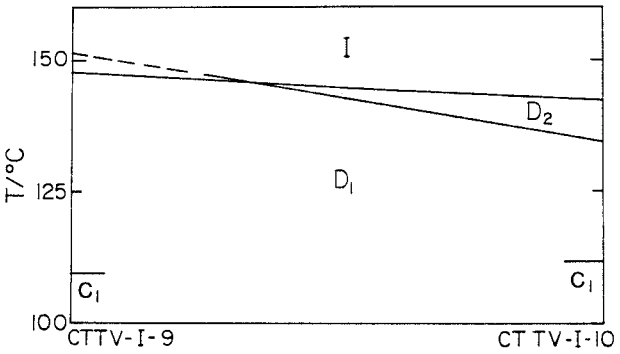

Figure 5. Binary phase diagram of CTTV-I-9 and CTTV-I-10. Note the triple D_1–D_2-I point at 146°C and the virtual D_1–D_2 transition for CTTV-I-9. The solid phases are not indicated in this diagram.

spindle joining the clearing temperatures of the two neat compounds is nearly straight and extremely narrow. The mesophase–mesophase transition line is almost parallel to the latter, as would be expected from the small enthalpy associated with this transition compared to that of the clearing enthalpy. The solubility curves and the dashed line, which represents the coexistence of the $n = 13$ crystals and the monotropic region of D_1, were calculated using the Le Chatelier–Schröder relation [20].

Figure 5 depicts a similar binary phase diagram for the $n=9$ and $n=10$ homologues (only the mesophase and liquid regions are shown). It establishes the isomorphism of the D_1 mesophases in the lower and higher homologues of the series. The triple D_1–D_2-I point in this diagram is observed at 146·0°C and by extrapolation (dashed line) [21] a virtual D_1–D_2 transition for neat CTTV-I-9 at 151·6°C can be calculated; this is almost 4°C above its clearing temperature (147·9°C). Since the enthalpies of the D_1 and D_2 mesophases in these compounds are similar, one could anticipate the formation of a supercooled uniaxial D_2 mesophase even in the lower members of the CTTV-I-*n* series.

3.1.3. *Deuterium NMR measurements*

In an attempt to obtain some information on the dynamic state of the mesophases, deuterium NMR measurements were performed on several members of the CTTV-I-*n* series. In figure 6, NMR spectra are presented for three isotopomers of CTTV-I-14, including compounds deuteriated in the unsubstituted aromatic sites (left), in the crown methylene (centre) and in the α-methylene of the side chains. The spectrum of the aromatic deuterons at 91°C (C_1) is typical of a rigid powder but, on increasing the temperature, broadening effects are observed indicating that already within C_1 some motion of the core moiety takes place. Further heating into the mesophase region (102°C) causes gradual changes typical of motional narrowing, but no discontinuities are detected at the transition between the two mesophases. Similarly, the crown deuterons exhibit a rigid powder spectrum in the crystalline C_1 phase (87°C) which undergoes gradual broadening on transforming to D_1 and D_2 (98°C, 109°C and 118°C). The α-methylenes are already mobile in the solid state phases C_2 (55°C) and C_1 (80°C) and undergo further motional narrowing within the mesophase region. A quantitative analysis of these results requires extensive comparison with simulated spectra which we have so far not done. It appears however that there is no correlation between the dynamics features of the spectra and the D_1–D_2 transition.

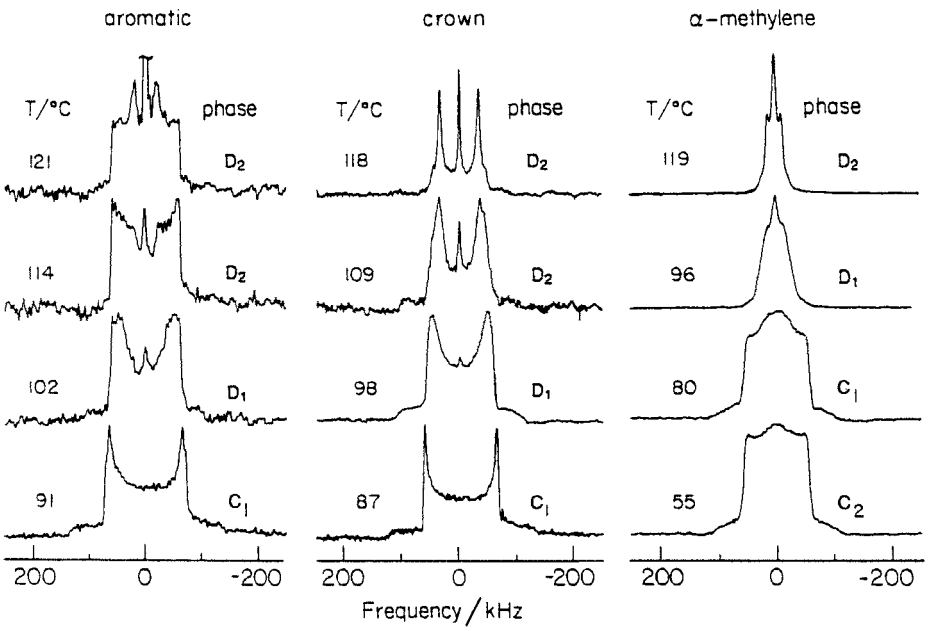

Figure 6. Deuterium NMR spectra of CTTV-I-14 deuteriated in the free aromatic sites (left), the crown methylenes (middle) and the α-methylenes of the side chains (right) at different temperatures in the solid and mesophase regions.

3.1.4. *X-ray diffraction*

More detailed information about the structure of the discotic mesophases was obtained from X-ray diffraction measurements. As indicated above, the lower homologues of the CTTV-I-*n* series ($n=5$ to 9) exhibit only one mesophase of which those for $n=6$ to 9 were measured. The X-ray patterns of all these compounds exhibit a very broad diffuse signal around $2\theta=15°$ to 25°, (3·5–6 Å), which is characteristic of scattering from disordered aliphatic chains and also, often corresponds to scattering from the intercolumnar stacking distances in discotic mesophases. On cooling to C_1 many new sharp peaks appear in the region of the diffuse peaks reflecting the setting-in of high intermolecular order. We therefore prefer to classify these phases as crystalline. For $n=6$ and 7, three more very weak peaks in the region $2\theta=5°$ to 8° are also observed (see figure 7 (*b*)). For $n=8$ and 9, a second much weaker diffuse peak is observed at $2\theta\sim12°$ (see figure 7 (*a*)) and for $n=9$ there is also a very weak narrow peak at $2\theta=7{\cdot}5°$. The sharp peaks in the region $2\theta=2°$ to 8° are due to scattering from the two dimensional arrangement of the columns. They cannot be indexed on an hexagonal lattice and were therefore preliminarily indexed on a general oblique lattice with a', b' and γ' as free parameters.

As representatives of the higher homologues ($n=10$ to 16), we show in figures 7 (*c*) and (*d*) the diffraction patterns for D_1 and D_2 of CTTV-I-13. Both patterns exhibit the diffuse signal at $2\theta\sim20°$, but the peak structure in the low angle region (2° to 8°) is quite different in the two phases. At 120°C (D_2), three peaks (one strong and two weak) are observed which can readily be indexed as the (10), (11) and (20) reflections of a two dimensional hexagonal lattice. At 92°C (D_1), the pattern is quite different, consisting of a strong doublet at $2\theta\sim3{\cdot}5°$ and several weak peaks around 5° to 8°. This pattern is very similar to that observed in the $n=6$ and 7 homologues and was again preliminarily

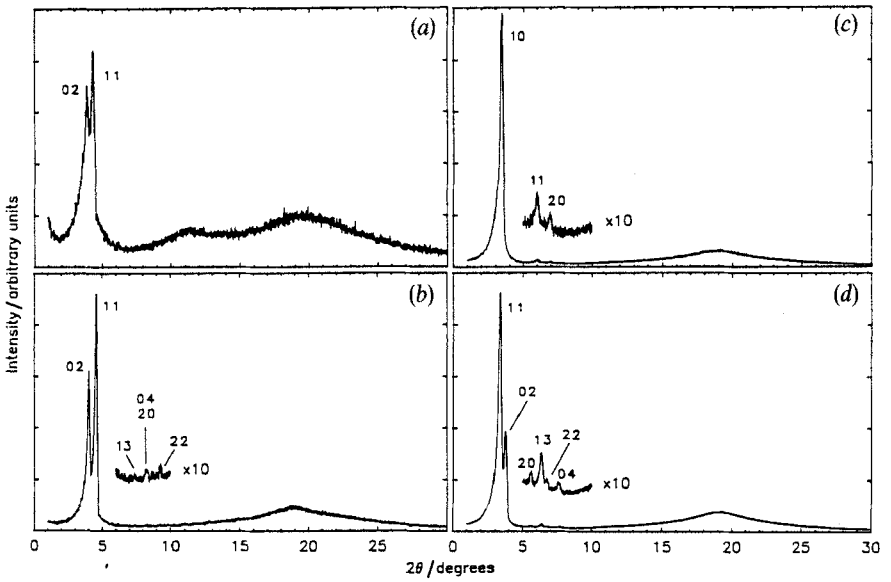

Figure 7. X-ray diffractograms of the discotic mesophases in some CTTV-I-*n* homologues. (*a*) CTTV-I-8, 134°C (supercooled D_1). (*b*) CTTV-I-7, 140°C (D_1). (*c*) CTTV-I-13, 120°C (D_1). (*d*) CTTV-I-113, 92°C (D_2). The assignment of the Miller indices is based on a hexagonal lattice for D_2 and a centred rectangular for D_1.

interpreted in terms of a two dimensional oblique lattice. Similarly distinct diffraction patterns with hexagonal and oblique symmetries were observed in the two mesophases of all the higher homologues ($n=10$ to 16) of the series. (In the $n=16$ homologue the stability range of D_1 is too narrow for reliable X-ray measurements to be made.)

Close examination of the diffraction data from the D_1 mesophases shows that the lattice parameters derived for the oblique unit cell are not independent and in fact are connected by the relation $a' = -2b' \cos\gamma'$, for all compounds. This indicates that the symmetry of the D_1 lattice is higher than oblique and corresponds to a centred rectangular unit cell with twice the area of the corresponding oblique cell. The measured d spacings and derived lattice parameters for the D_1 (rectangular) and D_2 (hexagonal) phases are summarized in tables 2(*a*) and (*b*), respectively. Assuming a density of approximately 1 g cm^{-3} there are two molecules and one molecule (columns) per unit cell in the two mesophases respectively. For several compounds, the lattice parameters were measured as function of temperature and, except, possibly near the D_1–D_2 transition, they remained fairly constant within each mesophase. The data reported in table 2 correspond to the middle region of the temperature range for the various phases.

The X-ray results for the D_2 mesophases are not sufficient for a distinction to be made between the five possible two dimensional hexagonal lattices. Such a distinction would require an analysis over more than just three reflections with the peak intensities included. It is most likely, however, that the molecules (columns) possess, on the average, cylindrical symmetry which would then imply an hexagonal p6mm unit cell (see figure 8).

With regard to the D_1 mesophases, we note that only reflections with Miller indices $h+k=$ even integers are observed. This limits the possible two dimensional lattices to just cm or c2mm (see figure 8) out of the seven possible rectangular unit cells. A

Table 2. (*a*) Measured and calculated *d* spacings and unit cell parameters for the rectangular mesophases, D_1, of the CTTV-I-*n* series†.

	Miller indices (*h k*)						Unit cell Parameters		Area
n	(0 2)	(1 1)	(1 3)	(2 0)	(0 4)	(2 2)	*a*	*b*	$a \times b$
6	20·1	18·0	11·2	10·1		9·0			
	(20·08)	(18·04)	(11·16)	(10·10)	(10·04)	(9·02)	20·19	40·16	811
7	21·4	18·9	11·8	10·6		9·5			
	(21·35)	(18·87)	(11·79)	(10·52)	(10·68)	(9·44)	21·04	42·71	899
8	22·3	20·1							
	(22·18)	(20·18)	(12·38)	(11·33)	(11·09)	(10·09)	22·66	44·36	1005
9	23·2	21·1		11·77					
	(23·42)	(21·05)	(13·02)	(11·79)	(11·71)	(10·53)	23·57	46·84	1104
10	23·9	22·0	13·5	12·3		11·0			
	(24·08)	(22·01)	(13·47)	(12·37)	(12·04)	(11·00)	24·74	48·17	1192
11	24·6	22·6	13·9	12·8		11·4			
	(24·66)	(22·68)	(13·82)	(12·77)	(12·33)	(11·34)	25·54	49·32	1260
12	25·3	23·9	14·4	13·4	12·8	11·8			
	(25·43)	(23·79)	(14·35)	(13·46)	(12·72)	(11·90)	26·92	50·86	1369
13	23·2	26·0	13·8	15·7	11·6	13·0			
	(23·23)	(25·95)	(13·88)	(15·65)	(11·62)	(12·98	31·29	46·46	1454
14	24·0	26·9	14·3	16·7					
	(23·87)	(27·05)	(14·32)	(16·41)	(11·97)	(13·52)	32·82	47·74	1567
15	24·7	27·2	15·0	16·4	12·4	13·6			
	(24·69)	(27·55)	(14·75)	(16·60)	(12·35)	(13·78)	33·20	49·38	1639

(*b*) Measured and calculated *d* spacings and unit cell parameters for the hexagonal mesophases, D_2, of the CTTV-I-*n* series†.

	Miller indices (*h k*)			Unit cell Parameter area	
n	(1 0)	(1 1)	(2 0)	*a*	$a^2\sqrt{(3)/2}$
10	22·8	13·1	11·4		
	(22·75)	(13·14)	(11·38)	26·27	598
11	23·4	13·6	11·8		
	(23·44)	(13·54)	(11·72)	27·07	635
12	24·5	14·2	12·2		
	(25·48)	(14·13)	(12·24)	28·27	692
13	25·2	14·6	12·6		
	(25·19)	(14·55)	(12·60)	29·09	733
14	26·2	15·3	12·9		
	(26·17)	(15·11)	(13·09)	30·22	791
15	27·0	15·5	13·4		
	(26·95)	(15·56)	(13·48)	31·12	839
16	27·5	15·9	13·7		
	(27·56)	(15·91)	(13·78)	31·82	877

† For each compound the first and second lines give the measured and (in parentheses) the calculated *d* spacings respectively. The units are in Angstroms and for computational purposes a precision of 0·01 Å was assumed.

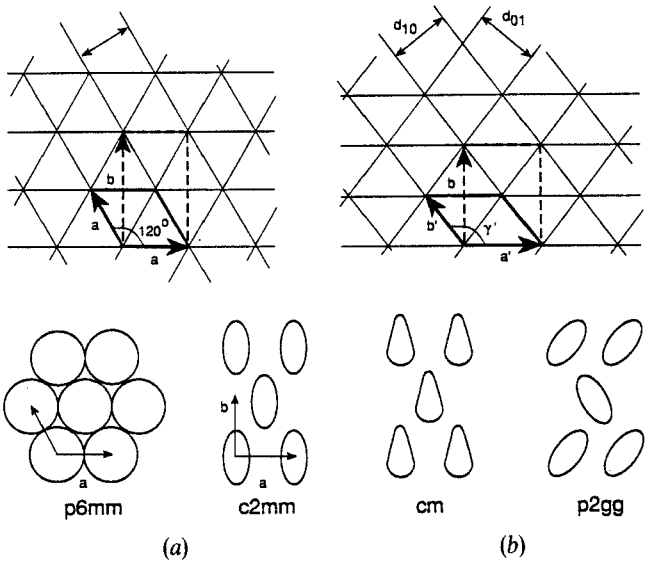

Figure 8. Top: Two dimensional hexagonal and rectangular lattices. a and b are lattice parameters for the hexagonal and rectangular unit cells, and a', b', γ' are the lattice parameters for the corresponding oblique cell. Bottom: Average columnar symmetries and schematic representations of p6mm, c2mm, cm and p2gg lattices.

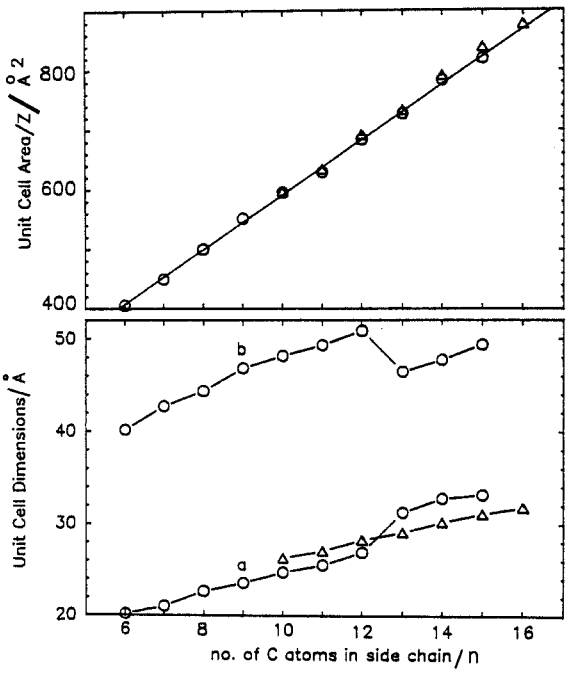

Figure 9. Average unit cell areas and lattice parameters for the hexagonal D_2 and rectangular D_1 mesophases as function of the number of carbons in the side chains of the CTTV-I-n series. The results correspond to approximately the middle of the mesophase stability range. D_1 (○) and D_2 (△).

distinction between these possibilities will again require an analysis of the peak intensities and probably a larger set of reflections than observed experimentally. However, a cm lattice is quite unlikely since it corresponds to molecules (columns) deformed into pear shapes (for example, by extending an uneven number of side chains in opposite directions) resulting in a (ferroelectric) mesophase with spontaneous electric polarization. On the other hand, we cannot absolutely rule out the possibility that D_1 is p2gg. The extinction conditions for this symmetry are that for the diffractions $h0$ ($0k$), h (k) must be even but $h+k$ for h, $k \neq 0$ can be both even or odd. If however, the deviation from c2mm symmetry is small, the diffraction peaks with $h+k=$ odd integers (for h, $k \neq 0$) are expected to be weak and perhaps undetectable. The first such diffractions for p2gg are 21, 12, 23 and 32. Such peaks were not observed at the expected 2θ values above the experimental noise level and we therefore tentatively identify the D_1 mesophases with c2mm symmetry.

The lattice parameters for the hexagonal (a) and rectangular (a, b) mesophases are plotted in figure 9 versus the number, n, of carbon atoms in the side chains. In general the cell dimensions increase monotonically with increase of the chain length, except that, for the D_1 mesophases, there appears to be a discontinuity on going from $n=12$ to 13. The formation of the c2mm phases can be viewed as an expansion or compression of the vertical dimension in the non-primitive rectangular unit cell of a hexagonal lattice (see figure 8). The discontinuity in the a and b curves in figure 9 thus reflects the fact that for $n=6$ to 12, the horizontal hexagonal layers expand, while for $n=13$ to 15 they compress relative to the corresponding spacing in the hexagonal lattice.

Also plotted in figure 9 are the average areas per molecule (area of the unit cell divided by the number of molecules per cell, $Z=2$ for c2mm, $Z=1$ for p6mm). The average molecular area increases essentially linearly with the number of carbons per side chain with a slope corresponding to 5·7 $Å^2$ per methylene group. In the compounds where both D_1 and D_2 exist, the average areas per molecule in the two phases is the same. This shows that the compression or expansion of the horizontal layers during the breaking of the hexagonal symmetry proceeds with a concomitant increase or decrease of the intermolecular distances within the layers, so as to keep the overall average molecular area fixed. The local symmetry of the molecules is apparently changed during the transformation from cylindrical in D_2 to elliptical in D_1. This could, for example, be brought about by extending an equal number of side chains in two opposite directions along the principal axes of the unit cells, or by tilting of the molecular planes about these axes. For the triphenylene esters it was shown by X-ray studies of strand mesophase samples [22] that the elliptical shape of the columns reflects such tilting of the molecular cores along the diagonals of the unit cells, resulting in a p2gg lattice.

3.1.5. *The nature of the D_1–D_2 transition*

Detailed temperature-dependent X-ray measurements were performed on the CTTV-I-13 homologue near the D_1–D_2 transition, at 2°C intervals between 90°C and 110°C and somewhat larger intervals outside this range. Expanded diffractograms in the region $2\theta=3°$ to 4°, recorded upon increasing the temperature, are depicted in figure 10. Similar patterns were obtained upon cooling, although slightly shifted (one to two degrees) temperature-wise. The diffractograms clearly indicate that over a wide temperature range, below the optically observed D_2–D_1 transition temperature (112·6°C), both phases coexist. Using the patterns recorded for the neat phases, the

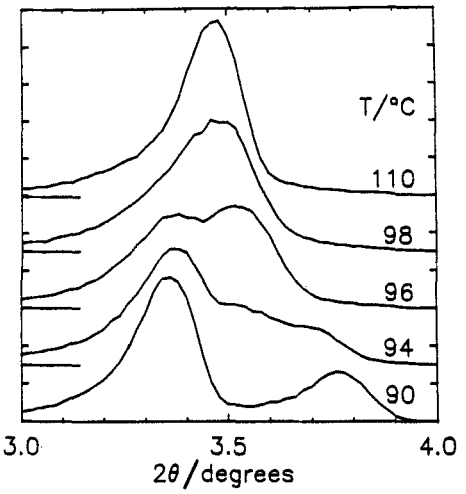

Figure 10. X-ray diffractograms of CTTV-I-13 in the region $2\theta = 3°$ to 4° at different temperatures near the D_1–D_2 phase transition region.

fractional population of $D_2$and D_1 in the coexistence region could be determined by comparison with the experimental diffractograms. In order to obtain a good fit to the experimental pattern, the positions of the diffraction peaks, as well as their relative intensities, must be allowed to vary somewhat, indicating that the lattice parameters may slightly change in the coexistence region. However, the general picture remains unchanged and shows that transformation between the two phases occurs over a temperature range of almost 20°C (92° to 110°C). The two phases are of equal abundance at about 97°C, i.e. 16°C below the optically observed D_2–D_1 transition.

The transition between the two mesophases is thus discontinuous, namely first order. The lack of a DSC peak is partly due to the wide range over which the transformation takes place, but it also indicates that the transition is only very weakly first order. The fact that a coexistence region is obtained both on cooling and upon heating is puzzling. It cannot be due to supercooling or superheating nor to slow kinetics of transformation. Impurity is a possibility, but unlikely, since the NMR spectra of the compound showed it to be of very high purity. Moreover, similarly wide coexistence regions were also observed in other members of the series ($n = 12$ and 14) which exhibit the D_1 and D_2 phases.

The nature of the hexagonal–rectangular transition in columnar phases was extensively investigated theoretically for thermotropic and lyotropic liquid crystals [23, 24]. The theories show that, depending on the details of the structures and energetics, the transition may be first or second order. The application of these theories to the D_1–D_2 transition in the CTTV-I-*n* series is an interesting topic which deserves further experimental and theoretical investigations.

3.1.6. *Miscibility with other compounds*

To compare the mesophases of the CTTV-I-*n* series with previously classified discotic mesophases [25, 26], we have constructed the binary phase diagram of the $n = 11$ homologue with a member of the hexalkanoyloxytriphenylene series having the

same side chains [27–32]. The phase diagram of the reference compound, *R* (hexaundecanoyloxytriphenylene) is

$$\text{Solid} \xrightarrow{67^\circ C} M_1 \xrightarrow{111^\circ C} M_2 \xrightarrow{122^\circ C} I$$

where M_2 and M_1 are hexagonal and centred rectangular (p2gg), respectively, and were classified as discotic D_B and D_A [25]. The binary phase diagram, shown in figure 11, indicates complete miscibility of M_2 with D_2 and of M_1 with D_1. There is a narrow miscibility gap between the two mesophases thus confirming the first order nature of the transition, and the complete miscibility between M_2 and D_2 confirms the hexagonal structure determined for D_2 by X-ray. The complete miscibility of M_1 and D_1 is more subtle. It may indicate that D_1 is after all p2gg with only a weak distortion from c2mm symmetry as discussed in connection with the interpretation of the X-ray data. Alternatively it could be that there is a Lifshitz line which is not observed by optical microscopy in the M_1–D_1 miscibility range with a second order transition between the p2gg phase of the reference compound and the c2mm phase of the $n = 11$ homologue. A distinction between the two possibilities could perhaps be made by X-ray measurements on monodomain samples.

Discotic mesophases can often sustain large amounts of non-mesogenic solvents, particularly consisting of flat aromatic molecules, such as benzene [9, 33–35]. To check whether similar behaviour applies to the D_2 and D_1 phases of the CTTV-I-*n* series, we studied the miscibility of one homologue ($n = 10$) with a less volatile aromatic compound, naphthalene. The binary phase diagram obtained from observation on contact preparations is shown in figure 12. The solidus curves in this diagram were calculated in four parts by the Le Chatelier–Schröder relation [20] as follows: the C_1 solubility curve was obtained from the melting data of CTTV-I-10 in table 1; the solubility curve for C_2 was calculated from the corresponding data for the virtual

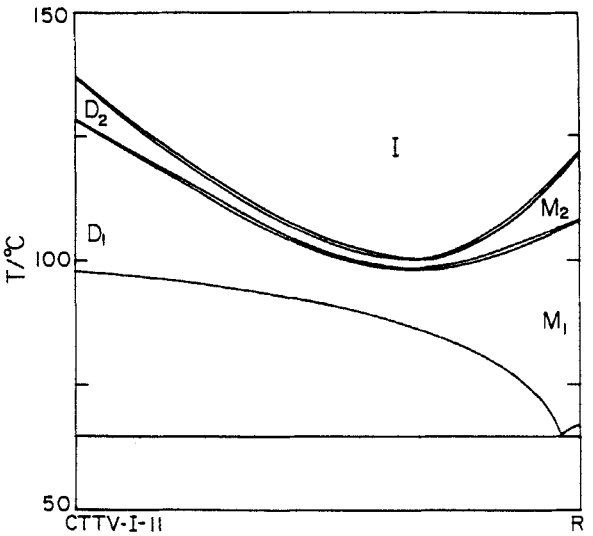

Figure 11. Binary phase diagram of mixtures of CTTV-I-11 (left) and the reference compound *R*, hexaundecanoyloxy 2,3,6,7,10,11-triphenylene (right). Only the liquid and the higher two mesophases are shown.

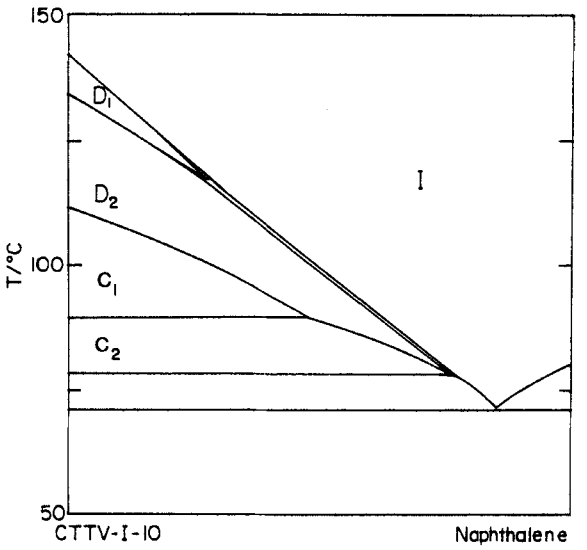

Figure 12. Binary phase diagram of mixtures of CTTV-I-10 (left) and naphthalene (right).

C_2–D_1 transition [21] (100·1°C; 69·2 kJ mol^{-1}). The solubility of the C_2 crystals was obtained from the virtual melting data on a 10 per cent solution (1°C, 84·5 kJ mol^{-1}), while the solubility curve of naphthalene was obtained from its own melting data (80·3°C; melting enthalpy 18·96 kJ mol^{-1} [36]). A eutectic temperature, calculated from these results to be at 71·5°C, is in good agreement with observation (71°C). The diagram shows that as much as 25 or 75 mol per cent of naphthalene can be dissolved in D_1 or D_2, respectively, before they become unstable at room temperature.

3.2. *Octaalkanoyloxyorthocyclophanes*

We have also extended our earlier work on the octaalkanoyloxyorthocyclophane series (CTTV-II-*n*). Four compounds were studied with $n = 12$, 14, 15 and 16. The phase diagrams of these mesophases are summarized in table 3. Each homologue exhibits only one mesophase which is, however, stable over a wide temperature range, from about 170°C for $n = 12$ to 130°C for $n = 16$. These mesophases for $n = 12$ and 14 were studied previously [5] by optical microscopy and were identified as columnar with uniaxial symmetry. Our present X-ray measurements are consistent with a columnar structure but indicate that the symmetry is biaxial. An example of an X-ray diffractogram for the $n = 12$ homologue is shown in figure 13. Five low angle scattering peaks can be discerned as well as a broad peak at $2\theta \sim 19°$, as was also observed in the ether series. Similar patterns were observed for the other CTTV-II-*n* homologues. They

Table 3. Phase transition temperatures (°C) for the CTTV-II-*n* series.

n	C		M		I
12	•	72	•	246	•
14	•	90	•	236	•
15	•	92	•	230	•
16	•	95	•	223	•

Table 4. Measured and calculated *d* spacings and unit cell parameters for the rectangular mesophase, D_r, of the CTTV-II-*n* series†.

	Miller indices (*h k*)						Unit cell Parameters		Area
n	(0 1)	(1 0)	(1 1)	(0 2)	(2 0)	(1 2)	*a*	*b*	$a \times b$
12	29·0	26·0	19·6	14·7	12·7				
	(29·40)	(26·00)	(19·48)	(14·70)	(13·00)	(12·80)	26·00	29·40	764
14	30·0	27·6	20·4	15·4	13·0				
	(30·05)	(27·12)	(20·13)	(15·03)	(13·56)	(13·14)	27·12	30·05	815
15	31·6	28·5	21·4	16·1	13·6				
	(31·55)	(27·99)	(20·94)	(15·78)	(14·00)	(13·74)	27·99	31·55	883
16	32·1	29·0	22·3	16·5	14·3				
	(32·25)	(29·00)	(21·56)	(16·13)	(14·50)	(14·09)	29·00	32·25	935

† For each compound the first and second lines give the measured and (in parentheses) the calculated *d* spacings respectively. The units are in Angstroms and for computational purposes a precision of 0·01 Å was assumed.

clearly cannot correspond to an hexagonal lattice as is evident for example by the splitting of the lowest angle diffraction peak. We have therefore attempted to index the diffractograms on a rectangular lattice and found a good fit within the experimental uncertainty. Hence we refer to these mesophases as discotic D_r. The lattice parameters so obtained are summarized in table 4 and are plotted as a function of the number of carbons in the side chains in figure 14. These results correspond to the low temperature range (up to about 50°C above the melting point) of the mesophase stability region. In this range the lattice parameters were found to be essentially independent of the temperature. Assuming a specific gravity of about 1 gr cm^{-3}, these results correspond to one molecule (column) per unit cell. A plot of the unit cell area as a function of the number of carbons in the chains shows a gradual increase with an average of 5·4 $Å^2$ per methylene groups, which is comparable with that found in the CTTV-I-*n* series (5·7 $Å^2$).

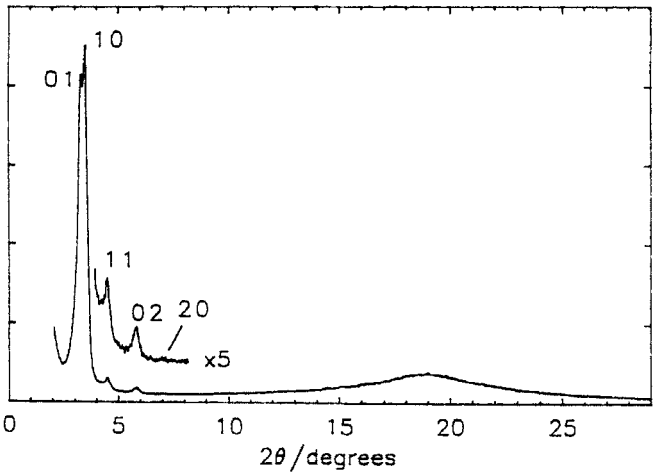

Figure 13. X-ray diffractogram of the D_r mesophase of CTTV-II-12 at 85°C. The assigment of the Miller indices is based on a rectangular lattice.

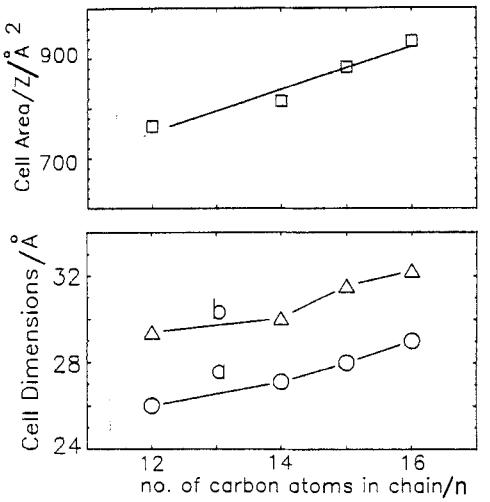

Figure 14. Average unit cell areas and lattice parameters for the D_r mesophases as a function of the number of carbons in the side chains in the CTTV-II-*n* series. The results correspond to the low temperature region of the mesophase stability range.

Comparison with the rectangular D_1 mesophase of the ether series shows that the biaxiality ratio, b/a, in the latter ranges between 1·4 and 2, while it is only 1·11 to 1·13 in the D_r phase of the ester series. This is perhaps the reason for not detecting the phase biaxiality by optical microscopy [5]. Based on the observed reflections (table 4) it may be concluded that the D_r mesophase can be assigned to either the p1ml or p2mm planar groups because all other rectangular planar groups require that one or both of the 10 or 01 reflections should be absent.

This work was supported by a grant from the G.I.F., the German–Israeli Foundation for Scientific Research and Development. We thank Professor Nguyen Huu Tinh for a sample of hexaundecanoyloxytriphenylene and Professor Shlomo Alexander for helpful discussions.

References

[1] Zimmermann, H., Poupko, R., Luz, Z., and Billard, J., 1985, *Z. Naturf.* (*a*), **40**, 149.
[2] Malthete, J., and Collet, A., 1985, *Nouv. J. Chem.*, **9**, 151.
[3] Levelut, A. M., Malthete, J., and Collet, A., 1986, *J. Phys., Paris*, **47**, 3571.
[4] Zimmermann, H., Poupko, R., Luz, Z., and Billard, J., 1986, *Z. Naturf.* (*a*), **41**, 1137.
[5] Zimmermann, H., Poupko, R., Luz, Z., and Billard, J., 1988, *Liq. Crystals*, **3**, 759.
[6] Zimmermann, H., Poupko, R., Luz, Z., and Billard, J., 1989, *Liq. Crystals*, **6**, 151.
[7] Bonsignore, S., Cometti, G., Dalcanale, E., and Du vosel, A., 1990, *Liq. Crystals*, **8**, 639.
[8] Abis, L., Arrighi, V., Cometti, G., Dalcanale, E., and Du vosel, A., 1991, *Liq. Crystals*, **9**, 277.
[9] Dalcanale, E., Du vosel, A., Levelut, A. M., and Malthete, J., 1991, *Liq. Crystals*, **10**, 185.
[10] Cometti, G., Dalcanale, E., Du vosel, A., and Levelut, A. M., 1990, *J. chem. Soc. Commun.*, p. 163; 1992, *Liq. Crystals*, **11**, 93.
[11] Kranig, W., Spiess, H. W., and Zimmermann, H., 1990, *Liq. Crystals*, **7**, 123.
[12] Percec, V., Cho, C. G., and Pugh, C., 1991, *J. mater. Chem.*, **1**, 217.
[13] Percec, V., Cho, C. G., and Pugh, C., 1991, *Macromolecules*, **24**, 3227.
[14] Percec, V., Cho, C. G., Pugh, C., and Tomazos, D., 1992, *Macromolecules*, **25**, 1164.

[15] MALINIAK, A., LUZ, Z., POUPKO, R., KRIEGER, C., and ZIMMERMANN, H., 1990, *J. Am. chem. Soc.*, **112,** 4277.
[16] POUPKO, R., LUZ, Z., SPIELBERG, N., and ZIMMERMANN, H., 1989, *J. Am. chem. Soc.*, **111,** 6094.
[17] SPIELBERG, N., LUZ, Z., POUPKO, R., PRAEFCKE, K., KOHNE, B., PICKARDT, J., and HORN, K., 1986, *Z. Naturf. (a)*, **41,** 855.
[18] GOLDFARB, D., LUZ, Z., SPIELBERG, N., and ZIMMERMANN, H., 1985, *Molec. Crystals liq. Crystals*, **126,** 225.
[19] ZIMMERMANN, H., 1989, *Liq. Crystals*, **6,** 591.
[20] LE CHATELIER, H., 1885, *C. r. hebd. Séanc. Acad. Sci., Paris*, **100**, 50. SCHRÖDER, T., 1893, *Z. phys. Chem.*, **11,** 449.
[21] DOMON, M., and BILLARD, J., 1975, *Pramana, Suppl.*, **1,** 131.
[22] SAFINYA, C. R., LIANG, W. A., CLARK, N. A., and ANDERSSON, G., 1984, *Phys. Rev. Lett.*, **53,** 1172.
[23] SUN, Y. F., and SWIFT, J., 1984, *J. Phys. Lett., Paris*, **45,** 509; 1984, *J. Phys., Paris*, **45,** 1801; 1986, *Phys. Rev.* A, **33,** 2745; 2740.
[24] CARTON, J. P., DUBOIS-VIOLETTE, E., and PROST, J., 1990, *Liq. Crystals*, **4,** 305.
[25] BILLARD, J., 1980, *Liquid Crystals of One and Two Dimensional Order*, edited by W. Helfrich and G. Heppke (Springer), p. 383.
[26] DUBOIS, J. C., and BILLARD, J., 1984, *Liquid Crystals and Ordered Fluids*, Vol. 4, edited by A. C. Griffin and J. F. Johnson (Plenum), p. 1043.
[27] DESTRADE, C., MONDON, M. C., and MALTHETE, J., 1979, *J. Phys., Paris*, **40,** C3-17.
[28] LEVELUT, A. M., 1980, *Liquid Crystals*, edited by S. Chandrasekhar (Heyden), p. 21.
[29] BILLARD, J., DUBOIS, J. C., VAUCHIER, C., and LEVELUT, A. M., 1981, *Molec. Crystals liq. Crystals*, **66,** 115.
[30] DESTRADE, C., TINH, N. H., GASPAROUX, H., MALTHETE, J., and LEVELUT, A. M., 1981, *Molec. Crystals liq. Crystals*, **71,** 111.
[31] LEVELUT, A. M., 1983, *J. Chim. phys.*, **80,** 149.
[32] TAKABATAKE, M., and IWAYANAGI, S., 1982, *Jap. J. appl. Phys.*, **21,** L685.
[33] CHANDRASEKHAR, S., SADASHIVA, B. K., SURESH, K. A., MADHUSUDANA, N. V., KUMAR, S., SHASHIDHAR, R., and VENKATESH, G., 1979, *J. Phys., Paris*, **40,** C3, 120.
[34] BILLARD, J., and SADASHIVA, B. K., 1979, *Pramana*, **13,** 309.
[35] GOLDFARB, D., LUZ, Z., and ZIMMERMANN, H., 1982, *J. Phys. Paris*, **43,** 421, 1255.
[36] TIMMERMANS, J., 1965, *Physico–Chemical Constants of Pure Organic Compounds*, Vol. 2, (Elsevier), pp. 131 and 133.